AGU PUBLICATIONS

JGR

Journal of Geophysical Research: Biogeosciences

RESEARCH ARTICLE
10.1002/2016JG003714

Key Points:
- Hot spots for accumulation and release of biogenic gas are identified in a subtropical peat soil at the submeter scale
- Heterogeneous distribution of gas accumulation and release is attributed to changes in physical properties of the peat matrix
- Appropriate spatial and temporal scale of measurement in gas flux studies is questioned

Correspondence to:
X. Comas,
xcomas@fau.edu

Citation:
Mustasaar, M., and X. Comas (2017), Spatiotemporal variability in biogenic gas dynamics in a subtropical peat soil at the laboratory scale is revealed using high-resolution ground-penetrating radar, *J. Geophys. Res. Biogeosci.*, *122*, 2219–2232, doi:10.1002/2016JG003714.

Received 14 NOV 2016
Accepted 10 AUG 2017
Accepted article online 14 AUG 2017
Published online 4 SEP 2017

Spatiotemporal variability in biogenic gas dynamics in a subtropical peat soil at the laboratory scale is revealed using high-resolution ground-penetrating radar

Mario Mustasaar[1] and Xavier Comas[2]

[1]Institute of Ecology and Earth Sciences, University of Tartu, Tartu, Estonia, [2]Department of Geosciences, Florida Atlantic University, Davie, Florida, USA

Abstract The importance of peatlands as sources of greenhouse gas emissions has been demonstrated in many studies during the last two decades. While most studies have shown the heterogeneous distribution of biogenic gas in peat soils at the field scale (sampling volumes in the order of meters), little information exists for submeter scales, particularly relevant to properly capture the dynamics of hot spots for gas accumulation and release when designing sampling routines with methods that use smaller (i.e., submeter) sampling volumes like flux chambers. In this study, ground-penetrating radar is used at the laboratory scale to evaluate biogenic gas dynamics at high spatial resolution (i.e., cm) in a peat monolith from the Everglades. The results indicate sharp changes (both spatially and temporally) in the dynamics of gas accumulation and release, representing hot spots for production and release of biogenic gases with surface areas ranging between 5 to 10 cm diameter and are associated with increases in porosity. Furthermore, changes in gas composition and inferred methane (CH_4) and carbon dioxide (CO_2) fluxes also displayed a high spatiotemporal variability associated with hot spots, resulting in CH_4 and CO_2 flux estimates showing differences up to 1 order of magnitude during the same day for different parts of the sample. This work follows on recent studies in the Everglades and questions the appropriateness of spatial and temporal scales of measurement when defining gas dynamics by showing how flux values may change both spatially and temporarily even when considering submeter spatial scales.

1. Introduction

Although peatlands only cover about 3% of the land and freshwater surface, they contain about one third of the carbon stored in the terrestrial biosphere [*Holden*, 2005]. Peatlands act both as a source of greenhouse gases, mainly by releasing methane (CH_4) and carbon dioxide (CO_2) to the atmosphere and as a carbon sink by sequestering atmospheric CO_2 [*Whiting and Chanton*, 2001]. However, the net effect (the difference between carbon emission and sequestration) of peatlands under changing climate conditions is currently uncertain [*Page et al.*, 2011; *Jauhiainen et al.*, 2012]. For that reason research in peatlands during the last two decades has focused on better quantifying biogenic gas emissions and its potential influence in climate change. Some of these studies have shown how biogenic gas accumulation and release in peat soils is strongly influenced by physical properties, such as peat type or environmental factors, such as temperature, water table depth, or atmospheric pressure [*Dise et al.*, 1993; *Shannon and White*, 1994; *Valentine et al.*, 1994; *Panikov and Dedysh*, 2000; *Kellner et al.*, 2005; *Coulthard et al.*, 2009]. For that reason peat development conditions as related to latitude (i.e., boreal versus subtropical) may influence biogenic gas dynamics, and therefore, the spatial distribution of biogenic gases within the peat matrix may vary considerably due to structural changes within the peat matrix in relation to changes in plant composition, porosity, organic content, or permeability of layers. *Rosenberry et al.* [2003] suggested that denser peat and regions with higher concentration of poorly decomposed plant remains (branches and roots) may favor bubble trapping and higher biogenic gas buildup. For that reason, certain physical properties (such as fiber distribution within the peat's matrix or degree of decomposition) may favor or prevent gas bubbles from escaping the peat and therefore influence its spatial distribution. These physical controls on gas distribution and release are supported by recent studies such as *Ramirez et al.* [2016], where variability in ebullition patterns in different peat soils is attributed to changes in peat structure.

During the last decade hydrogeophysical methods like ground-penetrating radar (GPR) have been used to investigate biogenic gas accumulation and release from peat soils both at the laboratory and the field

scales, proving GPR as an ideal method for noninvasively identifying areas of increased gas activity (i.e., hot spots) in peat soils. For example, in a study of a boreal peatland in Maine, *Comas et al*. [2011] detected variability exceeding 10% in gas content per volume attributed to changes in the internal structure of the peat matrix. Similar areas with increased gas content were described in an earlier work in the same peatland by *Comas et al*. [2005] and were attributed to the presence of hot spots of about 2–5 m wide and 1–2 m thick. Similar studies in boreal systems in Minnesota have shown 1–2 m thick areas of gas content reaching 25–30% in gas content that extended 10 to 100 m laterally as related to the presence of confining wood layers [*Parsekian et al*., 2011]. Other studies have shown the contrast between boreal systems in different latitudes (i.e., Maine versus Wales, UK), describing the presence of hot spots below wood layers in Maine (with differences exceeding 20% in gas content per volume), while nonexisting in Wales where gas distribution was more homogenous (i.e., consistent peat humification throughout a 7 m thick peat column) and wood layers were absent [*Comas et al*., 2013]. While these studies demonstrate the importance of changes in peat structure for defining hot spots of biogenic gas accumulation, it is important to note that (1) they are mostly field based and therefore imply transects of several tens or hundreds of meters that represent large measuring volumes ranging at scales between 100–1000 m^3 and (2) they are conducted almost exclusively in northern peatlands, while very few studies have been centered on tropical and subtropical peatlands [i.e., *Comas and Wright*, 2014; *Wright and Comas*, 2016] despite the fact that peat composition is different (i.e., *Sphagnum* peat in boreal system versus sawgrass or water lily peat in the Everglades). Given the heterogeneous nature of peat soils and the fact that different methods use different sampling volumes, it is important then to consider how smaller-scale variability may affect dynamics of biogenic gas accumulation within the peat matrix and release into the atmosphere and what is the spatial extent of hot spots in peat soils at smaller (i.e., submeter) scales and particularly for subtropical soils.

Since the presence or not of hot spots in a specific sampling volume will directly influence spatial variability in terms of gas dynamics, the timing and sampling interval for a specific measurement will also determine this variability. For example, recent studies in peat soils from the Everglades have shown increases in gas flux rates up to threefold larger when comparing hourly to daily scales [*Comas and Wright*, 2012, 2014]. While these studies question the appropriate temporal scale of measurement to properly capture dynamics of biogenic gas in peat soils, the extent of hot spots and its potential influence on spatial and temporal scales of measurement is still poorly understood. Therefore, it is important to understand how gas distribution in peat soils changes in relation to the presence (or absence) of areas of enhanced accumulation and/or release (i.e., hot spots) at smaller scales (i.e., submeter) that are more relevant for methods that use smaller sampling volumes like flux chambers.

The main aim of this paper is to investigate the spatial variability in biogenic gas accumulation and release in peat soils at high resolution (i.e., cm) and identify the presence (or not) of hot spots in a subtropical peat soil monolith using a combination of GPR, biogenic gas traps, and surface deformation rods. Variability in biogenic gas composition (i.e., CH_4 and CO_2 concentrations) is concurrently monitored using gas chromatography. The importance of scales of measurement (both spatial and temporal) for gas distribution (as different areas within the monolith may evolve differently over time) is also investigated. This study has therefore implications for better understanding carbon dynamics in subtropical peat soils (such as the Everglades) and for better defining the heterogeneous nature of hot spots of enhanced biogenic gas (i.e., CH_4 and CO_2) accumulation and release. This is particularly important when defining rates of gas release from subtropical systems that can be used as inputs for climate models.

2. Experimental Design and Methodology

A large peat monolith 0.53 m × 0.43 m × 0.30 m) was extracted from the Loxahatchee Impoundment Landscape Assessment (LILA) project which is an experimental wetland complex constructed at the Arthur R. Marshall Loxahatchee National Wildlife Refuge in Boynton Beach, Florida. Construction of the complex involved shifting of peat soils from one location to another within the impoundment; however, no offsite materials were brought in to the site [*Sklar et al*., 2004]. Therefore, and given its geographical location, soils at LILA correspond to Loxahatchee peat as defined by *Craft and Richardson* [2008] after *Gleason and Stone* [1994]. These peat soils are characterized by high organic content (up to 92%), and higher degree of decomposition (compared to other peat soils in the Everglades), and are originally formed from vegetation of

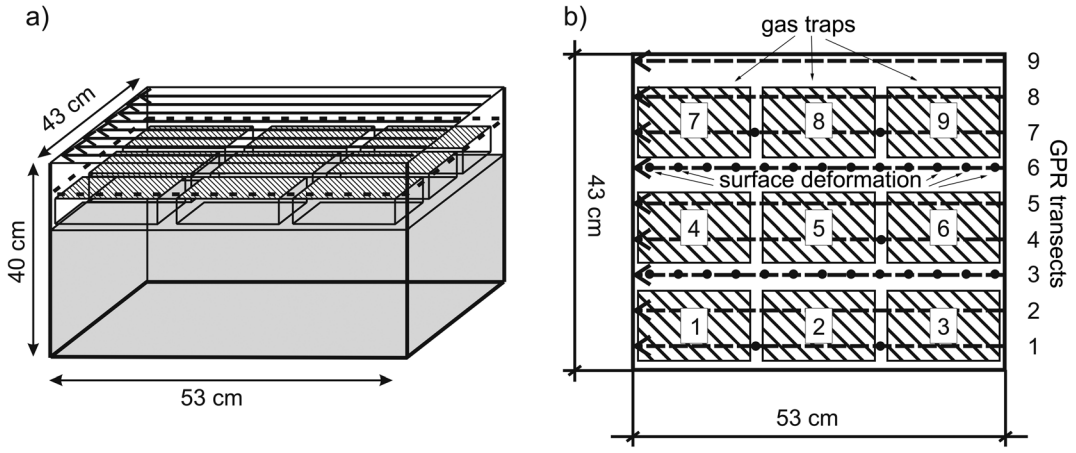

Figure 1. (a) Schematic showing the experimental setup. The dotted line marks water table, and the grey area represents the peat soil. (b) Setup view of the experiment setup showing the location of the nine gas traps. Dashed lines (numbered 1–9 on the right-hand side) mark the location of the GPR profiles, whereas the arrowheads indicate the profiling direction. The black dots denote the locations where surface deformation was measured.

sloughs (i.e., water lily or *Nymphaea odorata*). The site where the monolith was extracted from, was adjacent to a tree island, and was mostly dominated by *Panicum hemitomon* and *Sagittaria lancifolia*. Average peat thickness was 0.8 m, and the water table was about 0.35 m above the peat surface. Peat soil was moderately decomposed averaging H5–H6 in the von Post scale. The peat monolith was extracted by cutting and pulling back the surrounding peat and base of the block and transported to the laboratory where it was fitted into a plastic container. Deionized water with fluid conductivity matching field conditions (~308 μS m^{-1}) was added into the container until the sample was covered by approximately 15 cm of water in order to mimic field conditions. The water level was kept constant throughout the experiment (49 days total) by adding water with conductivity matching field conditions to compensate for water loss due to evaporation. In order to investigate the spatial distribution of gas flux and directly measure gas releases at different locations within the sample, nine individual gas traps (active footprint of 0.016 m^2) were installed and evenly distributed on the surface of the sample. Figure 1 shows both a three-dimensional diagram (Figure 1a) and a plan view (Figure 1b) displaying the dimensions and spatial distribution of gas traps (1–9), GPR transects (1–9), and location of peat surface deformation measurements. Traps (with dimensions 0.16 m × 0.10 m × 0.08 m) were constructed from clear plastic and were inverted, submerged into the water column, and floated above the peat's surface. Direct contact between the surface of the peat and the traps was avoided in order to prevent disturbance of the peat matrix and causing potential degassing.

GPR is a geophysical method that uses a transmitter to generate a pulse of electromagnetic waves that travel through the subsurface and returns to a receiver after reflecting from certain interfaces. Such interfaces represent contrasts in the dielectric permittivity (ε_r), the primary physical property that governs GPR, and are strongly dependent on water content [*Topp et al*., 1980]. In our study, we targeted changes in travel time to a reflector located at approximately 18 ns (two-way travel time) in a common offset profile interpreted as the bottom of our sample holder (i.e., peat-sample holder interface, Figure 2). Since the peat monolith was fully saturated, changes in travel time from the peat surface to reflector were only related to changes in biogenic gas content within the peat matrix as explained later. In the common offset mode, the transmitter and receiver are kept at a fixed distance and moved simultaneously across the transect. A total of nine GPR common offset profiles (line numbers indicated as 1–9 arrows in Figure 1b) separated 5 cm was collected by placing a shielded antenna at the cover of the sample holder. A Mala-RAMAC system equipped with 1.2 GHz antenna was used for all GPR measurements. A total of 34 traces per profile was collected using a trace spacing of 2 cm, a time window of 47 ns, and a stacking of 16 in order to improve signal-to-noise ratio. Six traces from the beginning and seven traces from the end of each profile were not considered due to container edge effects. Also, it is important to note, however, that each radar trace represents a sampling volume that resembles an elliptical cone with a base defined by an ellipse with 4.9 cm and 2.4 cm

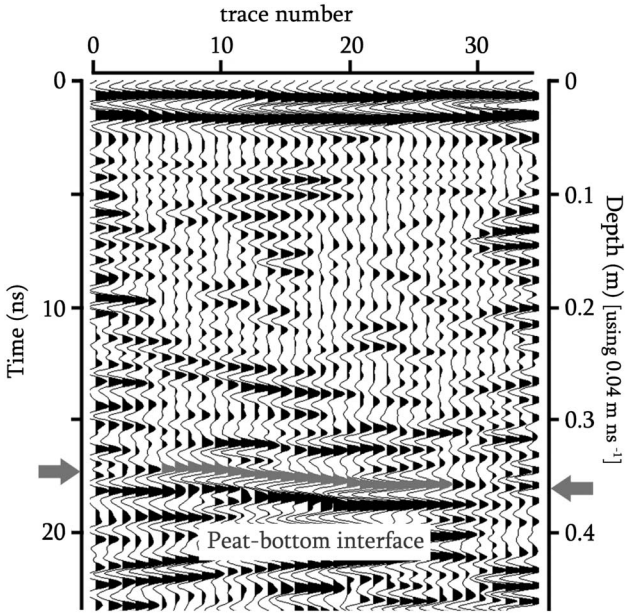

Figure 2. Typical common offset profile with interpreted peat-bottom interface.

radius at the bottom of the sample (as determined from the definition of radar-footprint size) [i.e., *Neal*, 2004]. Figure 2 shows an example GPR common offset profile where both individual traces and the interpreted peat-bottom interface can be observed. For each GPR survey (generally every 2–3 days), travel times to this particular reflector were picked at the peak of the first sidelobe of the reflected wavelet and an average velocity for the entire peat column was estimated using the thickness of the sample at each measurement location corrected for peat matrix deformation as later explained. Differences in travel time to the peat-bottom reflector reached values up to 1.26 ns between surveys.

Estimates of the average electromagnetic wave velocity (v) for the peat column at each measurement location and time were expressed in terms of dielectric permittivity assuming a low-loss medium with low magnetic permeability as follows:

$$\mathbf{v} = \frac{\mathbf{c}_0}{\sqrt{\boldsymbol{\varepsilon}_{\mathbf{r(b)}}}} \tag{1}$$

where c_0 is the electromagnetic wave velocity in vacuum (3×10^{-8} m s^{-1}) and $\varepsilon_{r(b)}$ is the bulk relative dielectric permittivity of the soil [*Davis and Annan*, 1989].

Calculated values of $\varepsilon_{r(b)}$ for each particular velocity were converted to gas content by applying the complex refractive index model (CRIM) [*Huisman et al*., 2003]:

$$\boldsymbol{\varepsilon}_{\mathbf{r(b)}}{}^{\boldsymbol{\alpha}} = \boldsymbol{\theta}\boldsymbol{\varepsilon}_{\mathbf{r(w)}}{}^{\boldsymbol{\alpha}} + (1-\mathbf{n})\boldsymbol{\varepsilon}_{\mathbf{r(s)}}{}^{\boldsymbol{\alpha}} + (\mathbf{n}-\boldsymbol{\theta})\boldsymbol{\varepsilon}_{\mathbf{r(a)}}{}^{\boldsymbol{\alpha}} \tag{2}$$

where $\varepsilon_{r(w)}$, $\varepsilon_{r(s)}$, and $\varepsilon_{r(a)}$ represent the relative dielectric permittivity values of water (temperature dependent and averaging 79.3 at 22°C for the entire sample), peat matrix [=2; as per *Comas et al*. [2005]) and air (=1), respectively; n is porosity (determined at the end of the experiment as explained below), θ is volumetric soil water content, and α is the index of anisotropy accounting for the orientation of the electromagnetic field and spatial distribution of peat fibers (typically 0.35 for peat soils as per *Kellner et al*. [2005]).

Errors in gas content measurements utilizing CRIM model arise from uncertainties of measured parameters (porosity and peat matrix deformation), predetermined values ($\varepsilon_{r(w)}$,$\varepsilon_{r(s)}$), and the empirical constant α. The error in gas content changes estimated from the CRIM model and based on propagation of errors [*Bevington*, 1969] reached values of ±1.4% when assuming errors of 0.5% for $\varepsilon_{r(w)}$, 0.5% for the electromagnetic wave velocity, 1.1% for porosity, and 2% for $\varepsilon_{r(s)}$ as per reported errors in *Comas and Wright* [2014]. Similar errors were estimated when considering variability in α between 0.35 and 0.5 (i.e., typical ranges in peat soils) [*Roth et al*., 1990; *Weitz et al*., 1997].

Surface deformation was monitored relative to a fixed datum (top of sample holder) by placing a graduated rod at selected locations as explained below and prior to each GPR measurement. Surface deformation was measured in a total of 31 locations distributed across the sample as follows: 13 points on line 3 and line 6, 2 points on line 1 and line 7, and 1 point on line 4 (Figure 1b). This distribution was based on area availability at the surface of the sample not covered by the gas traps described in Figure 1. This approach follows that described by *Price* [2003] and assumes that the change in thickness of the peat is caused by biogenic gas accumulation and release within the sample's matrix and that all change occurs only in the vertical direction

(i.e., no lateral displacement is considered). Estimated maximum error in all surface deformation measurements was 0.003 m.

Porosity was estimated as a weight difference between water saturated sample and oven dried sample for a cylindrical volume (3.2 cm long and 4.95 cm in diameter) extracted at selected locations. Although acquisition of at least one porosity measurement per gas trap location was initially intended, issues with soil collapse during extraction resulted in sample extraction in only six traps (traps 2, 3, 4, 7, 8, and 9). Peat samples for porosity measurements were extracted at about 7 cm from the surface. However, three samples at different depths were extracted underneath trap 7 to investigate how porosity may vary vertically within the peat monolith. Since the nature of these porosity measurements is destructive and therefore requires the extraction of a subsample of soil, porosity determination was performed only at the end of the experiment. Following the approach described in *Comas and Slater* [2007], the initial porosities for each particular data set over time (n_t) used in our CRIM model were adjusted relative to the measured value of final porosity (n_f) taking into account surface deformation as follows:

$$\mathbf{n_t} = \mathbf{n_f}\left(\frac{\mathbf{h_t}}{\mathbf{h_f}}\right) \tag{3}$$

where h_t and h_f denote the thickness of the peat on day t and at the final day, respectively. The final thickness of the peat was determined at each particular trace location where GPR measurements were performed (total of 176 GPR traces/thickness locations) by inserting a thin metal rod into the sample until resistance due to the bottom of the sample holder was noted. By adding the relative changes in surface deformation over time (as described above) to those final depths, thickness at each particular day (t) was estimated.

The gas accumulated in the traps was collected approximately every 2–3 days by submerging 2.4 mm ID Tygon tubing below the trap that was connected to a 60 mL syringe. Total volume at each trap was recorded, and extracted volumes were expressed in terms of fluxes by considering surface area (i.e., footprint of gas trap) and time between sample collection (i.e., sampling interval). Once extracted, gas content analysis for CH_4 and CO_2 was performed in triplicate using a SHIMADZU GC-8A gas chromatograph. Extracted volumes of CH_4 and CO_2 over time were used for estimating gas fluxes by considering surface area of gas traps. It is important to note that our gas content analysis was limited to carbon-based gases only, and therefore, other species were not analyzed (i.e., such as N_2 or O_2 as described in other studies investigating the composition of gas bubbles in the Everglades) [*Chanton et al*., 1988]. Atmospheric pressure and temperature was also measured in the laboratory using a HOBO Microstation data logger (with sampling interval of 5 min) with temperature and barometric pressure smart sensors.

3. Results

3.1. Temporal Variability in Overall Gas Dynamics

Overall variability in GPR gas content and fluxes for the entire peat monolith can be explored by calculating averages for both GPR-estimated gas content and entrapped gas volumes in the gas traps expressed as a gas flux. As previously explained, a total of 88 measurement distributed equally over the sample was used to calculate the average GPR gas content for the entire peat monolith (considering that a few centimeters along the edges were not included in the estimate as explained above) from surface to the bottom and for each day. Average GPR-estimated gas content within the peat matrix at the beginning of data collection was 8.5% and exhibited an overall decreasing trend for the remainder of the experiment, reaching 6.2% at the end of the experiment (average radar gas content for each day in bottom graph of Figure 3). By defining trends when more than two consecutive datapoints show a consistent increase or decrease in gas content, the overall temporal behavior can be divided into four major periods of gas content decrease within the peat matrix (periods I–IV shaded in grey in Figure 3) separated by periods of gas buildup (periods 1–4 shown in white in Figure 3). The first gas content decreasing period from day 0 to day 7 (I in Figure 3) is characterized by a gas content decrease from 8.48% to 7.28% (0.14% decrease per day), whereas the second major period of decrease in gas content (II in Figure 3) takes place between day 11 and day 14 and shows a gas content decrease from 7.45% to 6.85% (0.20% decrease per day). The noticeable gas content buildup event between days 14 and 18 with average rate of gas accumulation of 0.31% per day separates the second and the third period of gas content decrease (III in Figure 3). The third gas content period of decrease between days 18 and

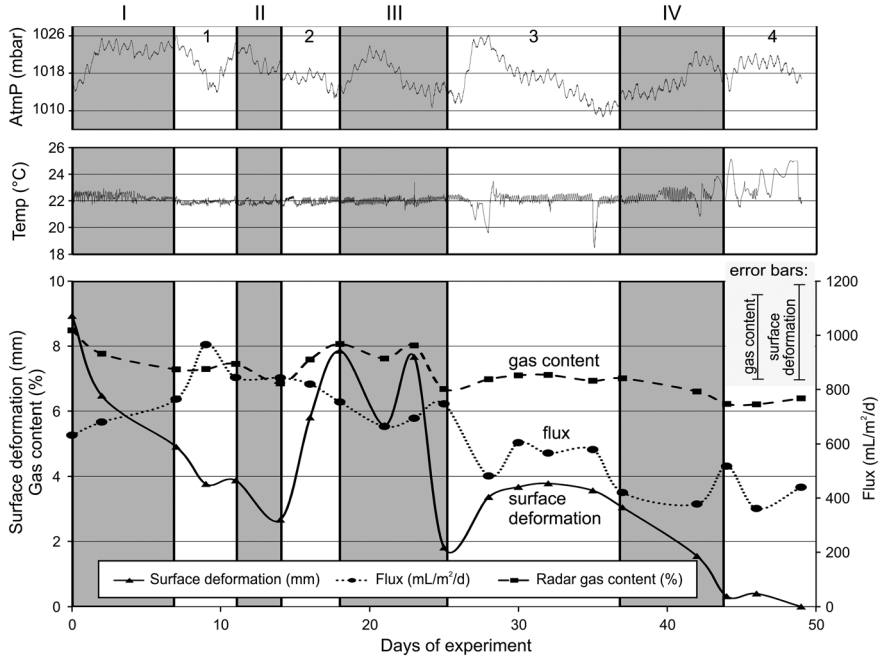

Figure 3. CRIM-estimated averaged gas content and gas flux estimated from gas traps for the whole peat block. Surface deformation of peat block averaged over all measurements, atmospheric pressure (AtmP), and air temperature (Temp) as a function of time is also shown. Grey areas indicate periods of decreasing gas content.

25 is characterized by a gas content decrease from 8.06% to 6.68% (0.2% decrease per day). During the fourth noticeable gas content decreasing period between days 37 and 44 (IV in Figure 3) the gas content decreases from 7.01% to 6.22% (0.11% decrease per day). Although it is important to consider that maximum-estimated errors in gas content may exceed 1% and thus be larger than some of these rates, we are confident on the validity of our measurements for two reasons: (1) the smoothness in trends for gas content variability, showing periods of increase and decrease with consecutive datapoints generating smooth slopes as opposed to random distributions; and (2) the fact that changes as later reported for individual traps are much larger and well above reported errors and show similar trends.

Overall gas flux averaged for the entire peat monolith was calculated by averaging estimated fluxes from all nine traps (flux in bottom graph of Figure 3). It is important to consider that while gas flux represents a cumulative measurement between days (i.e., value is a response of gas release during 2–3 days), GPR gas content represents a discrete measurement at each particular day (i.e., every 2–3 days) that should reflect those changes in flux release (i.e., periods of increased flux should result in lower gas contents). For that reason it seems reasonable to compare the two. Flux dynamics, similarly to GPR gas content, is characterized by a general decreasing trend from day 0 to day 49. A direct comparison between gas content and gas flux through regression analysis shows a weak but significant positive linear correlation with $R^2 = 0.35\%$ and P value <0.05. This correspondence is, however, counterintuitive when the two variables are plotted together over time (Figure 3), showing an overall increasing trend in flux release coinciding with periods I–IV (periods of gas content decrease) and an overall decreasing trend in flux release coinciding with periods 1–4 (periods of gas content increase). Surface deformation measurements show an opposite correspondence (when compared to flux) with periods I–IV characterized by an overall decrease in deformation and periods 1–3 showing an overall increase in deformation. For example, highest deformation (reaching almost 8 mm) coincides with high gas content and decreased flux values during period III, while low deformation coincides with the end of periods marked by decreasing trends in gas content (i.e., III and IV). Linear regression analysis reveals a statistically significant positive linear relationship between gas content and surface deformation (R^2 of 0.92 and P value <0.05).

Figure 3 also shows atmospheric pressure and temperature values during the experiment and their correspondence with periods I–IV and 1–4. Although a direct correspondence between changes in atmospheric

pressure and changes in gas content and/or flux cannot be derived from the data set, overall tendencies show periods of high atmospheric pressure during periods I, II, III, and IV. While temperature remains fairly constant throughout the experiment, some variability was recorded during periods 3 and 4. Linear regression analysis also reveals (1) a statistically significant negative linear correlation between air temperature (averaged during the period representing the flux measurement) and flux ($P < 0.05$) despite a low R^2 (0.24), thus indicating a weak correlation; (2) no statistical significant relationship between atmospheric pressure (averaged during the period representing the flux measurement) and gas flux ($P > 0.05$ and $R^2 = 0.12$) despite the fact that certain low-pressure events resulted in increased fluxes (i.e., Day 9, Day 25, Day 35, and Day 44 in Figure 3); and (3) no statistical significant relationship between atmospheric pressure (at the time gas content was measured) and gas content ($P > 0.05$ and $R^2 = 0.0006$).

3.2. Spatial Variability in Gas Dynamics Within the Peat Monolith

To further understand how GPR gas content and gas flux release may vary spatially within the peat monolith and investigate the presence and extent of hot spots for gas accumulation and release, we can consider the peat surface as split into nine areas coincident with the location of the nine gas traps and average the value of the traces coincident with the footprint of each particular gas trap (generally representing a total of 9 or 12 GPR traces, i.e., less traces in those areas influenced by edge effects). Figure 4 shows GPR gas content and gas flux for each particular trap (1–9). As shown in Figure 4, the highest calculated gas content values for a single region reached up to 13% (trap 3) at the beginning of the experiment whereas the smallest values were around 4% (traps 7 and 8). Gas content and flux values vary from trap to trap (e.g., gas content under traps 4 and 7 was mainly around 5% and 6%, whereas gas content under trap 3 stayed above 10% during the entire length of experiment). Overall spatiotemporal variability in gas flux values for the nine traps differ by more than 50 times and 2 orders of magnitude, i.e., the lowest flux for a 5 day period was 50 mL/m^2/d in trap 4, while the highest was 2625 mL/m^2/d in trap 9 (Figure 4). Gas flux measurements estimated from gas traps as shown in Figure 4 also reveal high temporal variability in gas releases (almost 1 order of magnitude). The maximum value of gas flux under trap 9 was 2625 mL/m^2/d, whereas under trap 4 the maximum calculated flux was 281 mL/m^2/d (almost 1 order of magnitude difference). Furthermore, a similar difference close to an order of magnitude also exists when comparing minimum values, i.e., 406 mL/m^2/d for trap 9 and 50 mL/m^2/d for trap 4. Linear regression analysis reveals a statistically significant positive linear correlation between gas flux and gas content for three traps: traps 2, 3, and 8, all showing $P < 0.05$ and $R^2 = 0.6$, 0.3, and 0.3 respectively, whereas a statistically significant negative correlation was noticed for trap 5 (R^2 0.37 and $P < 0.05$). Furthermore, it is important to consider that individual traps show different behaviors when comparing one to the other. For example, trap 5 shows an overall increase in flux values after day 28, while the rest of traps show either overall steady values or decreases.

To further investigate spatial variability in gas content and gas flux at finer spatial resolution, two-dimensional (2-D) plots of changes in gas content (relative to day 0) were generated for selected time periods. Static distribution of 2-D gas during the experiment reveals GPR gas content variability exceeding 4% over the 0.17 m^2 extent of the peat block, much larger than the estimated maximum errors of 1.4% reported earlier. Figure 5 depicts the 2-D distribution of gas content for day 0, followed by the change in gas content during days 14, 25, and 46 relative to day 0. Negative numbers indicate decreases in gas content relative to day 0. Color scale shows dark to light colors as indicative of smaller to larger decreases in gas content, respectively (and thus associated with smaller to larger flux, respectively). Gas content change relative to day 0 remains between 1.4 and 2.9% on selected days (as shown in Figures 5b–5d). Figure 5a depicts gas content distribution on day 0 with gas content variability of 4.5% and a trend of decreasing gas content from bottom right to top left (gas content decrease from 11.8% to 7.3%). The variability of gas content change relative to day 0 for each particular day ranges between 0.8% (on day 14 Figure 5b), 1% (on day 25 Figure 5c), and 1.2% (on day 46 Figure 5d). All selected days show a consistent preferential gas release location in the top right corner (Figures 5b–5d) with an approximate surface area of 5 cm by 5 cm that coincide with the location of trap 9 (which showed the highest flux values throughout the experiment as reflected in Figure 4). Regions with smaller gas content change relative to day 0 do not exhibit a regular pattern and concentrate along different locations during different days; however, representative dimensions are similar, for example, in the bottom left and in the central part of the sample on day 14 (coinciding with traps 1 and 4; Figure 5b), both with surface areas of about 5 cm by 5 cm, in the bottom part of the sample on day 25 (coinciding with

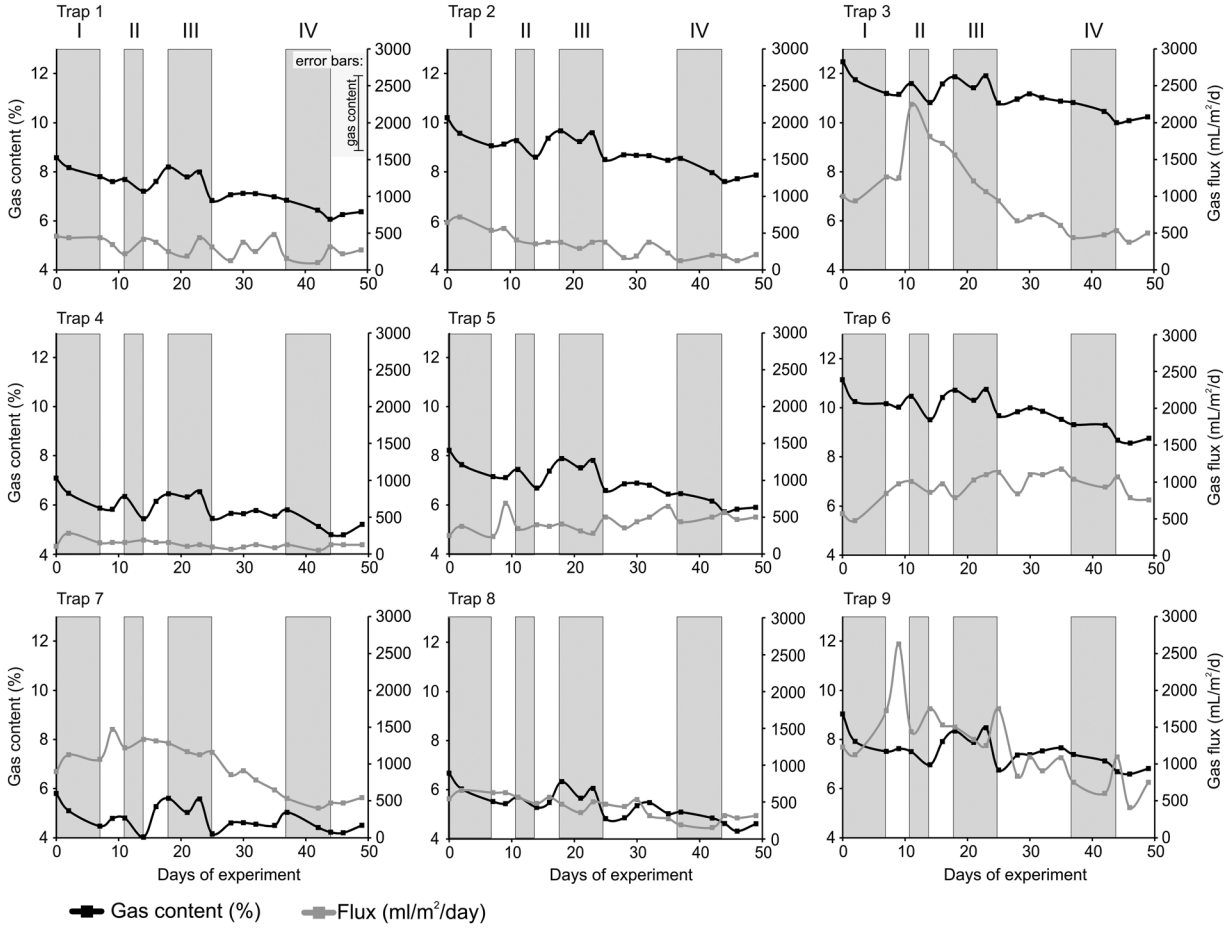

Figure 4. CRIM-estimated gas contents and gas fluxes as a function of time for equally spaced portions of the peat block. For trap locations see Figure 1. Estimated error in gas content is up to 1.4%.

traps 1, 2, and 3; Figure 5c) with representative surface areas of about 8 cm × 8 cm and in the top left part of the sample on day 46 (coinciding with trap 4; Figure 5d) with a representative surface area of about 10 cm × 5 cm.

3.3. Spatial and Temporal Variability in Gas Flux and Composition

Measured CH_4 and CO_2 flux values display high spatial and temporal variability as shown in Figures 6a and 6b. The highest CH_4 and CO_2 fluxes (852.8 and 179.5 mg/m^2/d, respectively) were recorded on day 14 of the experiment at trap 3, resulting from the highest gas volumes released but also due to the high CH_4 and CO_2 compositions (i.e., 71% CH_4 and 5.4% CO_2). Overall gas compositions throughout the entire experiment ranged between 9–77% CH_4 and 2.5–18% CO_2, with some gas traps consistently showing high values (i.e., traps 3 and 6 show values between 43–74% CH_4 and 3.4–18% CO_2), while others were characterized by consistently low values (i.e., traps 1 and 2 show values between 11–34% CH_4 and 3.2–7.2% CO_2). The variable nature of gas flux and composition over time is illustrated by the fact that some of the lowest CH_4 and CO_2 flux values were also recorded along trap 3 (as 33.3 and 12.2 mg/m^2/d, respectively, with gas compositions of 43% CH_4). The smallest flux values recorded under trap 3 are more than 1 order of magnitude lower than the highest values calculated from the same trap and show nearly half the composition recorded during high volume releases. Spatial variability in gas flux is also remarkable as revealed by the differences in flux values recorded on the same day from different parts of the sample. For example, on day 14 the difference in both maximum and minimum CH_4 and CO_2 values both exceeded 1 order of magnitude (i.e., CH_4 flux in trap 3 was 852.8 mg/m^2/d and 28.2 mg/m^2/d in trap 4, whereas CO_2 flux values from the same traps were 179.5 and 13.3 mg/m^2/d).

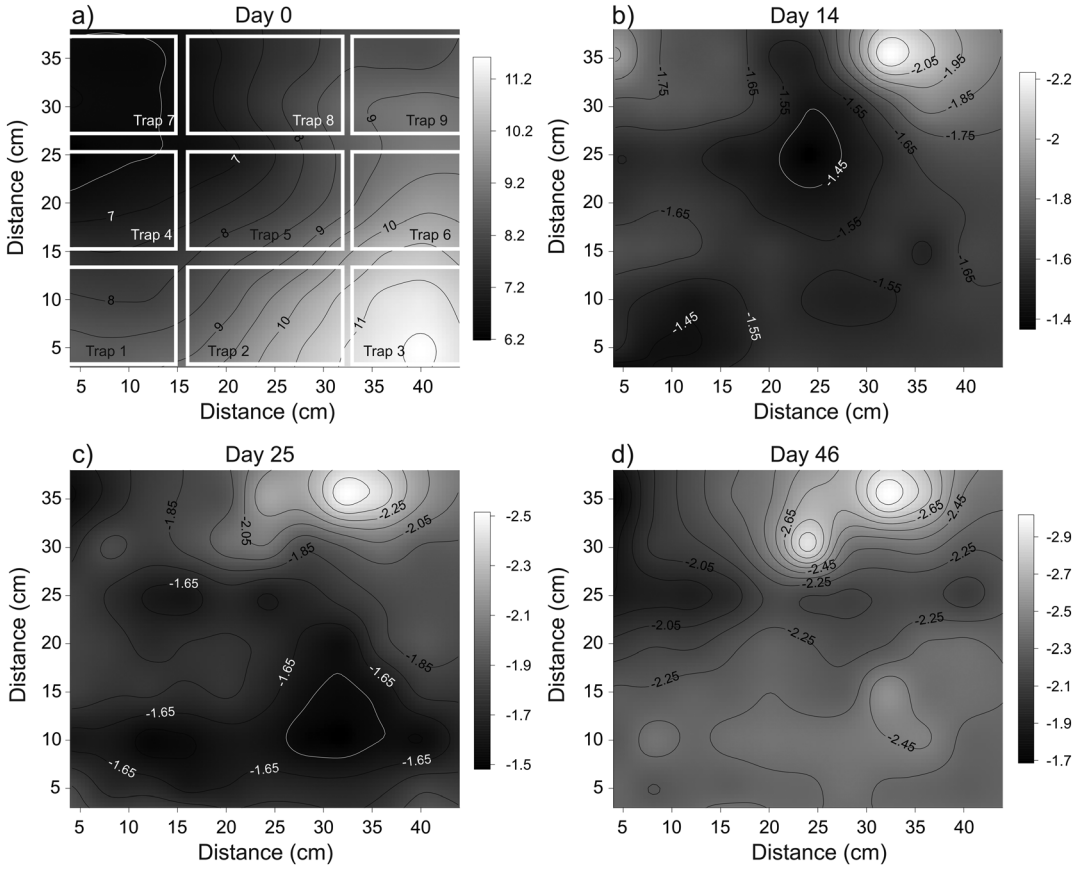

Figure 5. Gas content on day 0 and changes relative to (a) day 0, on (b) day 14, on (c) day 25, and on (d) day 46. Note the differences in color scales. Estimated error in gas content is up to 1.4%.

Figures 6a and 6b also reveal two marked periods of higher CH_4 and CO_2 flux values: one period between days 14 and 23 and the second period between days 44 and 46. These periods are separated by a marked low during day 37. It is important to note that the period of lower CH_4 and CO_2 flux around day 37 coincides with (1) an overall increasing trend in GPR gas content; (2) two lower temperature events on days 27 and 35 when temperature fell from room temperature (averaging 22°C) to 19.5°C and 18.5°C, respectively, due to malfunctioning of temperature controller; and (3) an overall period of decreasing atmospheric pressure (Figure 3).

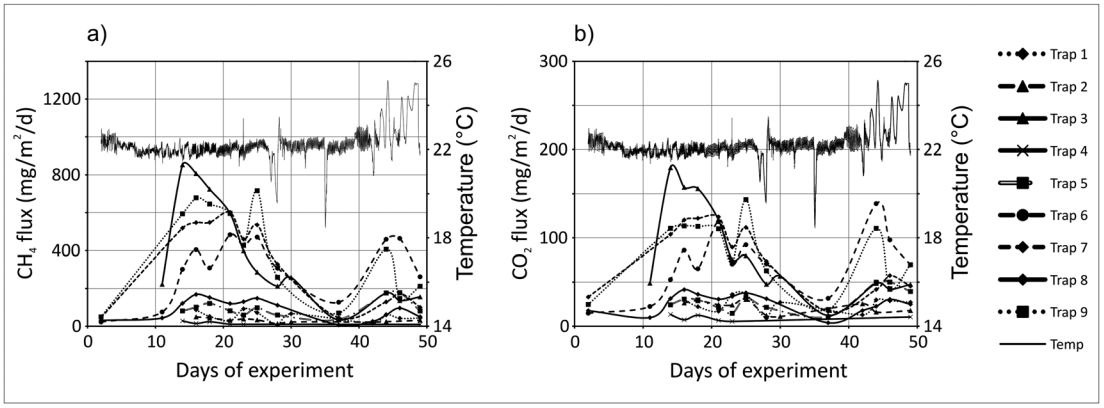

Figure 6. (a) CH4 flux in traps as a function of time and (b) CO_2 flux in traps as a function of time. Scale temperature is also shown as a secondary ax.

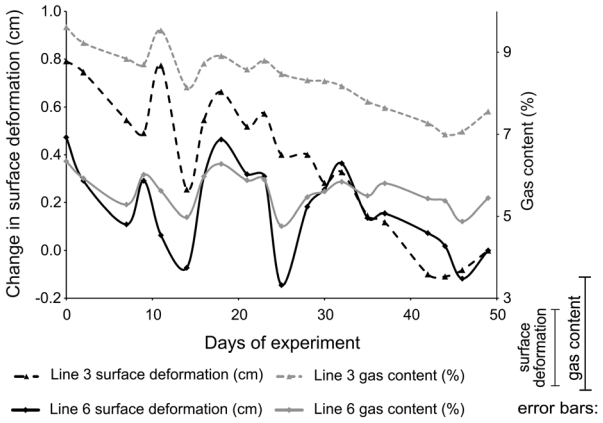

Figure 7. Change in surface deformation of line 3 and line 6 relative to last day and GPR-estimated gas content change along the same lines as a function of time. Locations of the lines are shown in Figure 1b. Maximum error for gas content is 1.4% and 0.3 cm for deformation.

3.4. Other Results: Surface Deformation, Porosity, and Atmospheric Pressure

Surface deformation data show consistent results when compared to the trends in gas content and fluxes. For the sake of brevity and to exemplify such trends, Figure 7 shows averaged surface deformation for line 3 and line 6 (see Figure 1b for location of the [1]transects) relative to the last day of the experiment. Both lines display decreasing trends from the beginning of the experiment, consistent with the decreasing trend in average radar gas content displayed in Figure 3 throughout the experiment. Spatiotemporal variability in surface deformation along the peat surface is well reflected from the difference in absolute values between the two lines, i.e., of surface deformation for line 6 is about half the values for line 3 for the first 32 days of the experiment. Figure 7 also reveals a strong correspondence between changing surface elevation and corresponding GPR gas content change in the soil. The prominent decrease in surface elevation (on day 14 and 25) and subsequent rise in surface elevation coincide with the contrasting gas content decreasing and increasing events along line 3 and line 6 during the same time.

Porosity measurements for all samples ranged between 89.3% and 93.9%. The highest porosity was recorded under trap 3 (93.9%), while the lowest porosity value was measured under trap 8 (89.3%). Traps 2, 4, and 9 recorded porosities of 91.6%, 93.0%, and 92.2%, respectively. Below trap 7 porosity values from the three different depths averaged 92.1% and showed the highest value in middle part of the sample (93.7%) and the top and bottom parts showing consistent values (91.0 and 91.4%, respectively). From these measurements, and although a clear correlation cannot be described from the limited amount of samples, it is important to note that (1) trap 3 showed the highest porosity while consistently recording both the highest flux an highest GPR gas content from all traps (Figure 4), (2) trap 8 showed the lowest porosity while recording one of the lowest flux and GPR gas content (Figure 4), (3) trap 7 shows a low GPR gas content while recording medium to high flux values when compared to the other traps, and (4) a final average porosity of 92.0% for the entire peat monolith was used for (a) correcting for surface deformation according to equation (3) and (b) calculating gas content according to the CRIM model in equation (2).

4. Discussion

The most striking observation from our study relates to the scattered distribution of hot spots for gas accumulation and release, ranging between 5 and 10 cm diameter in surface area at the laboratory scale explored here. Rate of gas accumulation and release observed within these hot spots changes both spatially and temporarily and is also characterized by variable gas composition. The presence of hot spots for gas production, accumulation, and release in peat soils has been suggested by others in boreal systems [i.e., *Waddington et al*., 1996; *Baird et al*., 2004; *Green and Baird*, 2013] and attributed to changes in peat type. We attribute these changes to small-scale (i.e., cm) variations in the physical properties of the peat matrix, which results in changes in behavior on how gas accumulates and gets released within the peat matrix. For example, in Figure 4, four different behaviors can be defined that relate gas dynamics to physical properties as follows: (a) relative high values for both gas content and flux (i.e., trap 3) indicate an area with enhanced gas accumulation (as supported by the highest porosity values, i.e., 93.9% in trap 3) that also result in large releases; (b) relative low values for both gas content and flux (i.e., trap 8) is indicative of low gas storage (as confirmed by the lowest porosity in trap 8, i.e., 89.3%) and release; (c) relative high values for gas content while fluxes are relatively low (i.e., trap 2 or 6) which may be indicative of increased ability to retain/store gas without

releasing it (unless gas has laterally migrated to adjacent traps); and (d) relative low values for gas content with overall high fluxes (i.e., trap 7), which are indicative of fast release and little storage (i.e., gas is released quickly after getting produced and without being stored).

While we acknowledge that our analysis of physical properties is solely based on changes in porosity, it is important to note that (1) recent studies [i.e., *Ramirez et al*., 2015, 2016] have demonstrated the importance of porosity for dictating gas dynamics in peat soils and how even a small difference in peat porosity (i.e., 2%) can produce large differences in patterns of gas storage and release (i.e., presence or not of diurnal production in the bubble flux); (b) changes in porosity across our peat monolith (up to 4.6%) match well the gas content variability estimated from the GPR (i.e., typically close to 5% difference in gas content as shown in Figure 5a); and (c) other physical changes within the matrix were noted at the end of the experiment, when the peat block was cut to extract samples for porosity measurements, such as the presence of a large root of *Eleocharis* under trap 8 that extended for 0.2 m across the sample. These structural changes within matrix may not only affect porosity (i.e., the lowest porosity values were detected below trap 8 and resulted in low gas content and flux) but also modify gas dynamics by channelizing underground gas flow to other areas in the monolith [*Ström et al*., 2003; *Ding et al*., 2005].

Furthermore, and as previously proposed by other studies on gas dynamics in subtropical peat soils [i.e., *Comas and Wright*, 2012, 2014], this study also shows how gas content and emission rates change when considering different spatial (i.e., sampling volume) and temporal scales of measurement. For example, biogenic gas content over time in our study varies from 6.4 to 8.5% when averaging for the entire peat monolith; however, gas content variability at a smaller scale (i.e., when dividing the peat monolith into nine sections) reveals a much larger variability in gas content (from 4 to 13%). This variability is related not only to overall gas content distribution in space and time but also in terms of gas composition as explained later. Changes in gas dynamics when considering different scales of measurement is also confirmed when examining gas flux values estimated from both gas traps and GPR. For example, gas flux values estimated from the gas traps for the entire peat monolith (i.e., Figure 3) vary widely and range between 361 and 965 mL/m^2/d. Flux estimates, however, become much more variable when considering individual gas traps (and thus a smaller scale of measurement when compared to averages for the entire peat monolith), ranging between 50 and 2625 mL/m^2/d (i.e., Figure 4), and showing an almost threefold increase in maximum values when considering smaller scales of measurement (individual traps compared to entire peat monolith). GPR flux (calculated as the change of gas content over entire volume of the peat monolith between two consecutive GPR gas content measurements, i.e., Figure 3) shows a single maximum value of 1957 mL/m^2/d followed by values below 1045 mL/m^2/d that are comparable to the larger-scale estimates from the traps. Similar to the gas traps, maximum gas fluxes estimated from the GPR measurements below individual traps (i.e., Figure 4) show much higher values up to 2363 mL/m^2/d.

Recent studies in the Everglades have shown similar flux results when comparing different temporal scales of measurement, both at the laboratory and field scales. For example, *Comas and Wright* [2012] estimated daily gas flux values from peat up to 287 mL/m^2/d at both laboratory and field scales, while hourly fluxes reached values up to 2468 mL/m^2/d in the laboratory. These results are strikingly similar to some of the fluxes in the present work although higher than previous studies in similar subtropical environments [i.e., *Happell et al*., 1993; *Whiting and Chanton*, 2001]. In a similar study in the Everglades *Comas and Wright* [2014] estimated hourly fluxes reaching values of more than 9000 mL/m^2/d and showing a threefold increase when compared to weekly estimates. Similar to the conclusions in these two studies [*Comas and Wright*, 2012, 2014], we also consider that the results presented here question the appropriateness of previous flux studies both in terms of spatial and temporal scales of measurement by showing how flux values may change depending on scale of measurement and time interval even when considering resolution at the cm scales.

Another striking observation from this study is the large spatial and temporal variability detected in gas composition during the length of the experiment. For example, CH_4 content in biogenic gas varied from 9% in trap 1 to 77% in trap 6 during the experiment. Although not as variable, CO_2 concentrations in gas varied from 2% in trap 4 to 18% in trap 6 which shows rates similar to the results obtained by *Chanton et al*. [1988]. These changes in concentration result in overall CH_4 flux values varying from 7 to 852 mg/m^2/d. The highest methane contents in the bubble correspond to four main traps (traps 3, 6, 7, and 9) with averages between 63 and 57% CH_4, which also correspond to the four locations with overall higher GPR-estimated gas

contents (Figure 4). This observation may indicate that these areas within the peat monolith not only are more efficient at accumulating biogenic gas but may also be hot spots for methane production. Previous studies have shown that plant-mediated CH_4 release (different than ebullition) from peat soils varies from 25% [*Morrissey et al*., 1993] to more than 90% [*Frenzel and Karofeld*, 2000] and depends mainly on dominant vegetation as well as climatic conditions. In our current work the inflow of water was absent and supply of fresh organic matter was limited by the existing vegetation remains contained within the sample and the root exudates produced by photosynthesis. While this limitation in inflow may be the reason for the overall decrease in gas content and gas flux release throughout the experiment, it will not explain the spatial and temporal variability in gas content, flux, and concentration. However, the spatial heterogeneity of CH_4 emission may be affected by the availability of substrate for methanogens which in turn is stimulated by the presence of roots [*Minoda and Kimura*, 1994; *Juutinen*, 2004]. Despite lacking a proper analysis of plant remains within the monolith, organic matter quality, or the changes in microbial population in this study, we attribute gas composition variability to a combination of factors including: (1) composition of plant species, (2) rhizospheric oxidation of CH_4 to CO_2 [*Ström et al*., 2005], and (3) difference in the quality of organic matter within the sample.

Linear regression analysis did not reveal a statistically significant relationship between atmospheric pressure (average atmospheric pressure between consecutive gas collections from gas traps) and gas flux. However, as previously described by *Comas et al*. [2007] for northern peatlands or *Comas and Wright* [2014] for subtropical peat in the Everglades and also revealed in Figure 3, several higher flux events can be corresponded with falling atmospheric pressure (i.e., on day 9, 25, and 44). *Tokida et al*. [2005] described a strong linear relationship between falling atmospheric pressure and CH_4 emission via ebullition. Figure 6 also supports the results obtained by *Tokida et al*. [2005] by showing higher CH_4 emissions on days 14, 25, and 44 during falling atmospheric pressure conditions. Figure 6 reveals also a prominent decrease in CH_4 emission on day 37 which occurs simultaneously with a lower atmospheric pressure period. Despite these observations, in order to properly describe the relationship between changing atmospheric pressure and flux, gas emission events should be measured using shorter time intervals i.e., using shorter intervals between gas extractions from gas traps or utilizing time-lapse cameras to autonomously estimate flux values from peat soils at subhourly time intervals as demonstrated by *Comas and Wright* [2012].

The laboratory-scale measurements presented here raise questions about the appropriate spatiotemporal scale of measurement when investigating carbon dynamics and biogenic gas emissions from peat soils in subtropical peatland systems such as the Everglades. Understanding the spatial and temporal distribution of hot spots for the accumulation and release of biogenic gases is critical when considering the need for realistic flux estimates from peat soils as input for global carbon budget calculations. While our study supports this understanding for small submeter scales, it is critical to expand these measurements to the field scale to better understand such variability for larger scales (i.e., meters to tens of meters). For example, in our current work a spatiotemporal variability up to 2 orders of magnitude in CH_4 flux values over a 0.17 m^2 peat sample was detected using gas traps with a footprint area of 0.016 m^2. Similarly, *Comas and Wright* [2012, 2014] found variabilities in biogenic gas fluxes several orders of magnitude larger when comparing daily measurements with hourly measurements in soils from the Everglades at both the laboratory and field scales. *Bartlett et al*. [1989] also described CH_4 flux variability of more than 1 order of magnitude in Everglades as dependent on ecosystem habitat. Although measurements in these studies were scattered within different peat soil types and did not explore the variability at the small scale (i.e., submeter) investigated in our study, these examples from both lab-scale and field-scale studies still question the appropriateness of current approaches for inferring gas fluxes from peat soils. As methodologies (such as eddy covariance) that involve large measurement footprints (often in the order of kilometers) have become more popular for carbon studies in peat soils during the last decade, it is important to keep in perspective the heterogeneous nature of carbon gas emissions from peat soils, particularly when considering the range in spatial and temporal variability of fluxes at much smaller scales as exemplified in this study.

5. Conclusions

In the work presented here, gas content estimated by GPR in conjunction with gas flux measurements from gas traps and surface deformation measurements reveals high spatial variability in gas content

(from 4 to 12%) and considerable spatiotemporal gas flux variations (from 50 to 2625 ml/m^2/d) within a 0.04 m^3 peat sample from the Everglades in the laboratory due to the scattered presence of hot spots for gas accumulation and release. These results stress the importance of sampling volume when investigating gas dynamics in peat soils by showing differences in flux estimates up to threefold when considering different scales of measurement. To achieve a better understanding of the gas accumulation and releasing patterns in peat soils, there is clear need for continuous data sets that will allow us to better temporarily constrain releasing events. The time-lapse camera approach by *Comas and Wright* [2012] shows promise; however, the potential for acquiring continuous automated GPR data sets may yield better understanding of the internal gas dynamics in peat soils and patterns of gas release at much shorter temporal scales (i.e., minutes) and larger sampling volumes (i.e., meters to tens of meters) that may help us better understand the presence and dynamics of hot spots at different scales and to better constrain emission rates from subtropical peatland systems to be incorporated into climate models.

Acknowledgments

This research was supported by European Social Fund's Doctoral Studies and Internationalisation Programme DoRa, which is carried out by Foundation Archimedes. The material is also based upon work partially supported by the National Oceanic and Atmospheric Administration (NOAA) under grant GC11-337 and the South Florida Water Management District and the U.S. Geological Survey (under the Greater Everglades Priority Ecosystems Science). We thank Eric Cline and LILA for all their support in the field. We also thank FAU graduate students William Wright, Greg Mount, and Matt McClellan for their help with laboratory work and field sampling. We also thank Editor Desai, David Nobes, and one anonymous reviewers for enhancing an earlier version of this manuscript. This manuscript is submitted for publication with the understanding that the United States Government is authorized to reproduce and distribute reprints for Governmental purposes. All raw data sets are available at http://www.geosciences.fau.edu/geophysics-lab/data-1.php or upon request from the author at xcomas@fau.edu.

References

Bartlett, D. S., K. B. Bartlett, J. M. Hartman, R. C. Harriss, D. I. Sebacher, R. Pelletier-Travis, D. D. Dow, and D. P. Brannon (1989), Methane emissions from the Florida Everglades: Patterns of variability in a regional wetland ecosystem, *Global Biogeochem. Cycles*, *3*(4), 363–374, doi:10.1029/GB003i004p00363.

Baird, A. J., C. W. Beckwith, S. Waldron, and J. M. Waddington (2004), Ebullition of methane-containing gas bubbles from near-surface *Sphagnum* peat, *Geophys. Res. Lett.*, *31*, L21505, doi:10.1029/2004GL021157.

Bevington, P. R. (1969), *Data Reduction and Error Analysis for the Physical Sciences*, McGraw-Hill, New York.

Chanton, J. P., G. G. Pauly, and C. S. Martens (1988), Carbon isotopic composition of methane in Florida Everglades soils and fractionation during its transport to the troposphere, *Global Biogeochem. Cycles*, *2*, 242–252, doi:10.1029/GB002i003p00245.

Comas, X., and L. Slater (2007), Evolution of biogenic gasses in peat blocks inferred from non-invasive dielectric permittivity measurements, *Water Resour. Res.*, *43*, W05424, doi:10.1029/2006WR005562.

Comas, X., and W. Wright (2012), Heterogeneity of biogenic gas ebullition in subtropical peat soils is revealed using time-lapse cameras, *Water Resour. Res.*, *48*, W04601, doi:10.1029/2011WR011654.

Comas, X., and W. Wright (2014), Investigating carbon flux variability in subtropical peat soils of the Everglades using hydrogeophysical methods, *J. Geophys. Res. Biogeosci.*, *119*, 1506–1519, doi:10.1002/2013JG002601.

Comas, X., L. Slater, and A. Reeve (2005), Spatial variability in biogenic gas accumulations in peat soils is revealed by ground penetrating radar (GPR), *Geophys. Res. Lett.*, *32*, L08401, doi:10.1029/2004GL022297.

Comas, X., L. Slater, and A. Reeve (2007), In situ monitoring free-phase gas accumulation and release in peatlands using ground penetrating radar (GPR), *Geophys. Res. Lett.*, *34*, L06402, doi:10.1029/2006GL029014.

Comas, X., L. Slater, and A. S. Reeve (2011), Atmospheric pressure drives changes in the vertical distribution of biogenic free-phase gas in a northern peatland, *J. Geophys. Res.*, *116*, G04014, doi:10.1029/2011JG001701.

Comas, X., N. Kettridge, A. Binley, L. Slater, A. Parsekian, A. J. Baird, M. Strack, and J. M. Waddington (2013), The effect of peat structure on the spatial distribution of biogenic gases within bogs, *Hydrol. Processes*, doi:10.1002/hyp.10056.

Coulthard, T. J., A. J. Baird, J. Ramirez, and J. M. Waddington (2009), Methane dynamics in peat: Importance of shallow peats and a novel reduced-complexity approach for modeling ebullition, in *Carbon Cycling in Northern Peatlands*, *Geophys. Monogr. Ser.*, vol. 184, edited by A. J. Baird et al., pp. 173–185, AGU, Washington, D. C., doi:10.1029/2008GM000811.

Craft, C. B., and C. J. Richardson (2008), Soil characteristics of the Everglades peatland, in *The Everglades Experiments: Lessons for Ecosystem Restoration*, edited by C. J. Richardson, pp 698–702, Springer, New York.

Davis, J. L., and A. P. Annan (1989), Ground-penetrating radar for high-resolution mapping of soil and rock stratigraphy, *Geophys. Prospect.*, *37*, 531–551, doi:10.1111/j.13652478.1989.tb02221.x.

Ding, W., Z. Cai, and H. Tsuruta (2005), Plant species effects on methane emissions from freshwater marshes, *Atmos. Environ.*, *39*, 3199–3207, doi:10.1016/j.atmosenv.2005.02.022.

Dise, N. B., E. Gorham, and S. Verry (1993), Environmental factors controlling methane emissions from peatlands in northern Minnesota, *J. Geophys. Res.*, *98*, 10,583–10,594, doi:10.1111/nph.12031.

Frenzel, P., and E. Karofeld (2000), CH_4 emission from a hollow-ridge complex in a raised bog: The role of CH_4 production and oxidation, *Biogeochemistry*, *51*, 91–112, doi:10.1023/A:1006351118347.

Gleason, P. J., and P. Stone (1994), Age, origin, and landscape evolution of the Everglades peatland, in *Everglades in the Ecosystem and Its Restoration*, edited by S. M. Davis and J. C. Ogden, pp. 149–197, St. Lucie Press, Delray Beach, Fla.

Green, S. M., and A. J. Baird (2013), The importance of episodic ebullition methane losses from three peatland microhabitats: A controlled-environment study, *Eur. J. Soil Sci.*, *64*, 27–36, doi:10.1111/ejss.12015.

Happell, J. D., J. P. Chanton, G. J. Whiting, and W. J. Showers (1993), Stable isotopes as tracers of methane dynamics in Everglades marshes with and without active populations of methane oxidizing bacteria, *J. Geophys. Res.*, *98*(D8), 14,771–14,782, doi:10.1029/93JD00765.

Holden, J. (2005), Peatland hydrology and carbon release: Why small-scale process matters, *Philos. Trans. R. Soc., A*, *363*, 2891–2913, doi:10.1098/rsta.2005.1671.

Huisman, J. A., S. S. Hubbard, J. D. Redman, and A. P. Annan (2003), Measuring soil water content with ground penetrating radar: A review, *Vadose Zone J.*, *2*, 476–491.

Jauhiainen, J., A. Hooijer, and S. E. Page (2012), Carbon dioxide emissions from an *Acacia* plantation on peatland in Sumatra, Indonesia, *Biogeosciences*, *9*, 617–630, doi:10.5194/bg-9-617-2012.

Juutinen, S. (2004), Methane fluxes and their environmental controls in the littoral zone of boreal lakes, Univ. of Joensuu, PhD dissertations in Biology, 110.

Kellner, E., J. M. Waddington, and J. S. Price (2005), Dynamics of biogenic gas bubbles in peat: Potential effects on water storage and peat deformation, *Water Resour. Res.*, *41*, W08417, doi:10.1029/2004WR003732.

Minoda, T., and M. Kimura (1994), Contribution of photosynthesized carbon to the methane emitted from paddy fields, *Geophys. Res. Lett.*, *21*, 2007–2010, doi:10.1029/94GL01595.

Morrissey, L. A., D. B. Zobel, and G. P. Livingston (1993), Significance of stomatal control on methane release form *Carex*-dominated wetlands, *Chemosphere*, *26*, 339–355, doi:10.1016/0045-6535(93)90430-D.

Neal, A. (2004), Ground-penetrating radar and its use in sedimentology: Principles, problems and progress, *Earth Sci. Rev.*, *66*, 261–330.

Page, S. E., J. O. Rieley, and C. J. Banks (2011), Global and regional importance of the tropical peatland carbon pool, *Global Change Biol.*, *17*, 798–818, doi:10.1111/j.1365-2486.2010.02279.x.

Panikov, N. S., and S. N. Dedysh (2000), Cold season CH_4 and CO_2 emission from boreal peat bogs (West Siberia): Winter fluxes and thaw activation dynamics, *Global Biogeochem. Cycles*, *14*(4), 1071–1080, doi:10.1029/1999GB900097.

Parsekian, A., X. Comas, L. Slater, and P. Glaser (2011), Geophysical evidence for the lateral distribution of free phase gas at the peat basin scale in a large northern peatland, *J. Geophys. Res.*, *116*, G03008, doi:10.1029/2010JG001543.

Price, J. S. (2003), Role and character of seasonal peat soil deformation on the hydrology of undisturbed and cutover peatlands, *Water Resour. Res.*, *39*(9), 1241, doi:10.1029/2002WR001302.

Ramirez, J. A., A. J. Baird, T. J. Coulthard, and J. M. Waddington (2015), Ebullition of methane from peatlands: Does peat act as a signal shredder?, *Geophys. Res. Lett.*, *42*, 3371–3379, doi:10.1002/2015GL063469.

Ramirez, J. A., A. J. Baird, and T. J. Coulthard (2016), The effect of pore structure on ebullition from peat, *J. Geophys. Res. Biogeosci.*, *121*, 1646–1656, doi:10.1002/2015JG003289.

Rosenberry, D. O., P. H. Glaser, D. I. Siegel, and E. P. Weeks (2003), Use of hydraulic head to estimate volumetric gas content and ebullition flux in northern peatlands, *Water Resour. Res.*, *39*(3), 1066, doi:10.1029/2002WR001377.

Roth, K., R. Schulin, H. Flühler, and W. Attinger (1990), Calibration of time domain reflectometry for water content measurement using a composite dielectric approach, *Water Resour. Res.*, *26*(10), 2267–2273, doi:10.1029/WR026i010p02267.

Shannon, R. D., and J. R. White (1994), A three-year study of controls on methane emissions from two Michigan peatlands, *J. Ecol.*, *84*, 239–246, doi:10.1007/BF00002570.

Sklar, F. H., et al. (2004), Ecological effects of hydrology, in *Everglades Consolidated Report South Florida Water Management District*, chap. 6, pp. 6–58, West Palm Beach, Fla.

Ström, L., A. Ekberg, M. Mastepanov, and T. Røjle Christensen (2003), The effect of vascular plants on carbon turnover and methane emissions from a tundra wetland, *Global Change Biol.*, *9*, 1185–1192, doi:10.1046/j.1365-2486.2003.00655.x.

Ström, L., M. Mastepanov, and T. R. Christensen (2005), Species-specific effects of vascular plants on carbon turnover and methane emissions from wetlands, *Biogeochemistry*, *75*, 65–82, doi:10.1007/s10533-004-6124-1.

Tokida, T., T. Miyazaki, and M. Mizoguchi (2005), Ebullition of methane from peat with falling atmospheric pressure, *Geophys. Res. Lett.*, *32*, L13823, doi:10.1029/2005GL022949.

Topp, G. C., J. L. Davis, and A. P. Annan (1980), Electromagnetic determination of soil water content: Measurements in coaxial transmission lines, *Water Resour. Res.*, *16*(3), 574–582, doi:10.1029/WR016i003p00574.

Valentine, D. W., E. A. Holland, and D. S. Schimel (1994), Ecosystem and physiological controls over methane production in northern wetlands, *J. Geophys. Res.*, *99*(D1), 1563–1571, doi:10.1029/93JD00391.

Waddington, J. M., N. T. Roulet, and R. V. Swanson (1996), Water table control of CH_4 emission enhancement by vascular plants in boreal peatlands, *J. Geophys. Res.*, *101*(D17), 22,775–722,785, doi:10.1029/96JD02014.

Weitz, A. M., W. T. Grauel, M. Keller, and E. Veldkamp (1997), Calibration of time domain reflectometry technique using undisturbed soil samples from humid tropical soils of volcanic origin, *Water Resour. Res.*, *33*(6), 1241–1249, doi:10.1029/96WR03956.

Whiting, G. J., and J. P. Chanton (2001), Greenhouse carbon balance of wetlands: Methane emission versus carbon sequestration, *Tellus B*, *53*, 521–528, doi:10.1034/j.1600-0889.2001.530501.x.

Wright, W., and X. Comas (2016), Estimating methane gas production in peat soils of the Florida Everglades using hydrogeophysical methods, *J. Geophys. Res. Biogeosci.*, *121*, 1190–1202, doi:10.1002/2015JG003246.